Emberson, R., Galy, A., Hovius, N. (2018): Weathering of Reactive Mineral Phases in Landslides Acts as a Source of Carbon Dioxide in Mountain Belts. - *Journal of Geophysical Research*, *123*, 10, pp. 2695—2713.

DOI: http://doi.org/10.1029/2018JF004672

Journal of Geophysical Research: Earth Surface

RESEARCH ARTICLE
10.1029/2018JF004672

Weathering of Reactive Mineral Phases in Landslides Acts as a Source of Carbon Dioxide in Mountain Belts

R. Emberson[1,2,3], A. Galy[4], and N. Hovius[1,5]

[1]GFZ Deutsches Geoforschungszentrum, Potsdam, Germany, [2]Now at Universities Space Research Association/GESTAR, Columbia, MD, USA, [3]Now at Hydrological Sciences Laboratory, NASA Goddard Space Flight Center, Greenbelt, MD, USA, [4]CRPG-CNRS-UL, Nancy, France, [5]Institute of Earth and Environmental Science, University of Potsdam, Potsdam, Germany

Key Points:
- Landsliding elevates dissolution of highly reactive mineral phases in rapidly eroding mountain belts
- In Taiwan, this process leads to extensive dissolution of sulfides and carbonate rock
- The net effect is to release carbon dioxide, inverting the commonly assumed negative feedback on chemical weathering via higher erosion

Supporting Information:
- Supporting Information S1
- Data Set S1

Correspondence to:
R. Emberson,
robert.a.emberson@nasa.gov

Citation:
Emberson, R., Galy, A., & Hovius, N. (2018). Weathering of reactive mineral phases in landslides acts as a source of carbon dioxide in mountain belts. *Journal of Geophysical Research: Earth Surface*, *123*, 2695–2713. https://doi.org/10.1029/2018JF004672

Received 8 MAR 2018
Accepted 6 OCT 2018
Accepted article online 12 OCT 2018
Published online 27 OCT 2018

Abstract Bedrock landsliding in mountain belts can elevate overall chemical weathering rates through rapid dissolution of exhumed reactive mineral phases in transiently stored deposits. This link between a key process of erosion and the resultant weathering affects the sequestering of carbon dioxide through weathering of silicate minerals and broader links between erosion in active orogens and climate change. Here we address the effect on the carbon cycle of weathering induced by bedrock landsliding in Taiwan and the Western Southern Alps of New Zealand. Using solute chemistry data from samples of seepage from landslide deposits and river discharge from catchments with variable proportions of landsliding, we model the proportion of silicate and carbonate weathering and the balance of sulfuric and carbonic acids that act as weathering agents. We correct for secondary precipitation, geothermal, and cyclic input, to find a closer approximation of the weathering explicitly occurring within landslide deposits. We find highly variable proportions of sulfuric and carbonic acids driving weathering in landslides and stable hillslopes. Despite this variability, the predominance of rapid carbonate weathering within landslides and catchments where mass wasting is prevalent results at best in limited sequestration of carbon dioxide by this process of rapid erosion. In many cases where sulfuric acid is a key weathering agent, a net release of CO_2 to the atmosphere occurs. This suggests that a causal link between erosion in mountain belts and climate change through the sequestration of CO_2, if it exists, must operate through a process other than chemical weathering driven by landsliding.

Plain Language Summary There is a long-standing debate surrounding the link between erosion and climate. It is often suggested that as temperatures increase, rainier and stormier weather could increase erosion of rock; as that rock is exposed, silicate minerals within could break down, which, on long time scales, can remove CO_2 from the atmosphere, lowering global temperatures and acting as a negative feedback. Recent studies have shown that landslide deposits are key locations for the link between chemical weathering and physical erosion in some mountain belts. To test how landslides affect the erosion-climate link, we used samples of water seeping through landslides in Taiwan and New Zealand to calculate the amount of carbon dioxide that is either absorbed or released through this chemical reaction. We find that the large amount of freshly exposed rock in Taiwanese landslide deposits contains significant carbonate rock and sulfide minerals; the net result of the weathering of these minerals is a release of carbon dioxide, which inverts the traditional perspective on the role erosion plays in controlling carbon dioxide release. In some mountain belts, it seems that increased erosion and resulting landsliding may act to increase carbon dioxide in the air, opening further questions into the nature of erosional-climatic links.

1. Introduction

High local weathering rates in landslide deposits have been shown to be a significant control on large scale solute fluxes from actively eroding mountain belts (Emberson et al., 2016). The physical effect of deep-seated landslides is to excavate and shatter fresh rock mass and generate deposits with an extremely high internal surface area (e.g., Casagli et al., 2003), facilitating rapid weathering. The impact of elevated rates of dissolution in landslides on the sequestration of carbon dioxide through silicate weathering remains unconstrained. This sequestration is important for long-term climatic cycles (Raymo et al., 1988; Raymo & Ruddiman, 1992), and determining the role of landslides in such geochemical cycling could help understanding of the effect of rapid erosion on climate. The form and strength of this connection remains a topic of open research (e.g., Millot et al., 2002; Riebe et al., 2004; West et al., 2005; Willenbring & von Blanckenburg, 2010); here we

address the explicit role of bedrock landslides, the chief process of erosion in steep uplands with high rates of denudation (Hovius et al., 1997).

Elevated weathering rates require either an increase in soluble material or an increased supply of acid, or both, since the concentration of carbonic acid in rainfall is limited by the partial pressure of CO_2 in the atmosphere (Galy & France-Lanord, 1999). Globally, soil respiration is the key process driving the increase in carbonic acid that is ultimately responsible for the rock weathering through percolation (e.g., Amundson, 2001). Soils are destroyed during landslides and weathering in bedrock landslide deposits, which involves exfiltration of fluids percolating though the landslide body with characteristically high solute concentrations, requires excess acid, but the process by which this is produced remains unclear. Landsliding disrupts and mixes soil, unweathered rock (e.g., Adams & Sidle, 1987; Geertsema & Pojar, 2007), and large organic debris (Hilton et al., 2011). The decay of fossil organic matter from bedrock and recent surface and soil derived material could serve as a source of carbonic acid. Moreover, bedrock landslides can excavate deep bedrock material from tens of meters below the saprolite-rock interface (Larsen et al., 2010), exposing highly labile phases such as sulfides and petrogenic organic carbon for rapid oxidation. The resultant sulfuric and carbonic acids are potent weathering agents (Emberson et al., 2016).

In this study, our aim is to calibrate the impact of rapid weathering in landslide deposits on the sequestration of carbon dioxide. To quantify this, we need to estimate not only the initial sources of acid in the weathering environment but also the balance of dissolved substrate, whether carbonate or silicate. Recently published work (Torres et al., 2016) has demonstrated that mountain belts can act as net sources of CO_2 to the atmosphere through sulfuric acid-driven weathering of carbonates. We test the hypothesis that the potential for rapid weathering of labile sulfides in fresh deposits of bedrock landslides (Emberson et al., 2016) could lead to landslides acting as a chief source of carbon dioxide to the atmosphere in mountain belts where sulfide minerals and carbonates coexist. In such settings carbonic and sulfuric acids are the two main weathering acids (e.g., Calmels et al., 2007; Galy & France-Lanord, 1999; Torres et al., 2016) and so we restrict our analysis accordingly.

We present measurements of major dissolved elements and measurements of the carbon isotopic composition of the dissolved inorganic carbon ($\delta^{13}C_{DIC}$) in seepage from a number of landslide deposits and small tributaries in two catchments in the rapidly eroding mountains of Taiwan, as well as catchments in the Western Southern Alps of New Zealand (WSA). Seepage refers to fluid exfiltrating at the surface of landslide debris. It is most often found at the terminal end of landslide deposits but may also occur upslope, where the local water table intersects the deposit surface. The initial source for the exfiltrating water, whether directly from precipitation or from deeper groundwater, is not clear in most cases, but focused sampling of landslide seepage can isolate the effect of this specific geomorphic process when considered at a catchment scale.

To calculate the balance of acid in these samples we use the carbon isotope ratios in dissolved inorganic carbon ($\delta^{13}C_{DIC}$), and the proportion of sulfate to bicarbonate, defined as XSO_4^{2-}:

$$XSO_4^{2-} = 2x\left[SO_4^{2-}\right]/\left(2x\left[SO_4^{2-}\right] + \left[HCO_3^{-}\right]_{total}\right)\ (Eq\%), \quad (1)$$

where $[SO_4^{2-}]$ is the concentration of sulfate in the solution and $[HCO_3^{-}]_{total}$ is the total amount of dissolved bicarbonate. The value obtained for XSO_4^{2-} is measured in percentage of Equivalents (Eq%). XSO_4^{2-} and $\delta^{13}C_{DIC}$ depend on the relative proportions of either silicate or carbonate weathering driven by one or other acid source. They also depend in part on several other factors, including deep degassing of metamorphic CO_2, cyclic (atmospheric) input, and combined postweathering degassing and precipitation of secondary calcite, which we correct for in turn to provide first order estimates of the initial balance of solvent acids and dissolved substrate. We refer to this as the weathering state. The postweathering effects (anthropogenic or cyclic input, secondary precipitation, and associated degassing) are corrected for using major element concentrations in catchment-derived suspended sediment, following methods outlined by Bickle et al. (2015) and Albarede (1995). The solid phase chemistry is also used to establish the end-member values for carbon isotope ratios required to model degassing.

Following these corrections, we use modeling of the end-member "initial" weathering scenarios, either silicate or carbonate weathering via either sulfide-derived sulfuric acid or carbonic acid from atmospheric sources or organic material decay, to derive the initial balance of acids that generated the final measured

values. Using this acid balance, we compare landslide seepage with local streams to assess how the sources of acid for weathering vary between landslides and subcatchments unaffected by mass wasting. In the WSA we lack good constraints on secondary factors that affect $\delta^{13}C_{DIC}$ and XSO_4^{2-} and as such the corrections are more limited; nevertheless, further insights are provided into the sources of acid in mass wasting-derived deposits.

We show that the sources of acid driving the intense weathering in recent bedrock landslides are not significantly different from those in catchments primarily draining soil-mantled regimes. However, the higher proportion of carbonate weathering in landslides results in a net output of carbon dioxide from dissolution in Taiwanese landslide deposits. The results from Taiwan are supported by measurements from New Zealand, where, despite lower levels of sulfide oxidation, the sequestration of CO_2 by silicate weathering in landslides is limited.

2. Study Sites

For this study, we sampled seepage from deposits of recent and older (up to 20 years since initial activation) landslides and rivers in two Taiwanese mountain catchments: the 370-km^2 Chenyoulan River catchment in the center-west of the island and the 119-km^2 Taimali River catchment in the southeast (Figure 1). Both catchments are typical of the Taiwanese orogen, both geomorphically and lithologically. The island of Taiwan is the site of some of the highest erosion rates (Dadson et al., 2003; Fuller et al., 2003) and weathering rates (Calmels et al., 2011; Carey et al., 2006) anywhere on the planet, as a result of the convergence of the Philippine Sea and Eurasian plates and the associated fast crustal shortening (Yu et al., 1997). The lithological makeup of the Taiwan Central Range is defined by the tectonic history; as an inverted passive margin, it is composed of variably metamorphosed sediments with significant fraction of carbonate (Chang et al., 2000; Ho, 1986). This is similar to many actively eroding mountain belts, but the erosion driven by active tectonics is enhanced by frequent typhoon-style rainfall. The ambient subtropical climate is likely to encourage rapid decomposition of organic matter (Kirschbaum, 1995).

Erosion rates are typically high (3–7 mm yr^{-1}, Dadson et al., 2003; Willett et al., 2003); both catchments have been affected by dramatic recent erosional events; in the Chenyoulan catchment, the 1999 Chi-Chi earthquake generated significant mass wasting, although short-term erosional perturbations have decayed to a background level (Hovius et al., 2011). The Taimali catchment was strongly impacted by Typhoon Morakot (in 2009), which produced approximately 25,000 landslides in southern Taiwan (Lin et al., 2011). Limited anthropogenic influence makes these catchments good settings in which to study the weathering within landslides. In both catchments a high degree of local variability exists between some tributary streams in terms of the landslide density; some subcatchments remained relatively untouched, allowing comparison of sources of acid between these unaffected areas and the seepage from landslides. To understand how the individual landslides scale up, we can also compare the modeled weathering in catchments with limited mass wasting to those where landsliding is significant, with $>$10% of the total area affected in some cases.

Lithologically, the Chenyoulan catchment is made up of Oligocene meta-sandstones and slates, while the Taimali catchment is formed of Miocene slate/shale (Central Geological Survey, M. of E. A., 2000). These are representative of the majority of the Tertiary sedimentary cover dominating the south and west of Taiwan. There is an abundance of marine sourced carbonate in the sedimentary bedrock in both catchments. Pyrite is an important minor component of Taiwanese lithologies, and its oxidation dominates the fluxes of dissolved sulfate in southern rivers (Das et al., 2012).

The carbon isotope data from the WSA are measured from samples that formed the basis of a previous study (Emberson et al., 2016), and the sampling locations are published therein. These New Zealand isotope samples are also from landslide seepage and catchments with variable degrees of landsliding. Briefly, the rivers of the WSA drain a fast uplifting (9 ± 4 mm yr^{-1}, Norris & Cooper, 2001) mountain belt made up of the silicate-rich Alpine Schist, with high precipitation (up to 12 m yr^{-1}, Henderson & Thompson, 1999) giving rise to high rates of erosion by landsliding (Hovius et al., 1997). Generally lower concentrations of solutes in rivers in the WSA compared to Taiwan (Carey et al., 2006) are the result of lower carbonate concentrations. The rivers are generally undersaturated with respect to calcite (e.g., Jacobson et al., 2003), reducing the complexity of the correction for secondary processes. Unlike Taiwan, however, we lack data to fully describe the carbon isotope

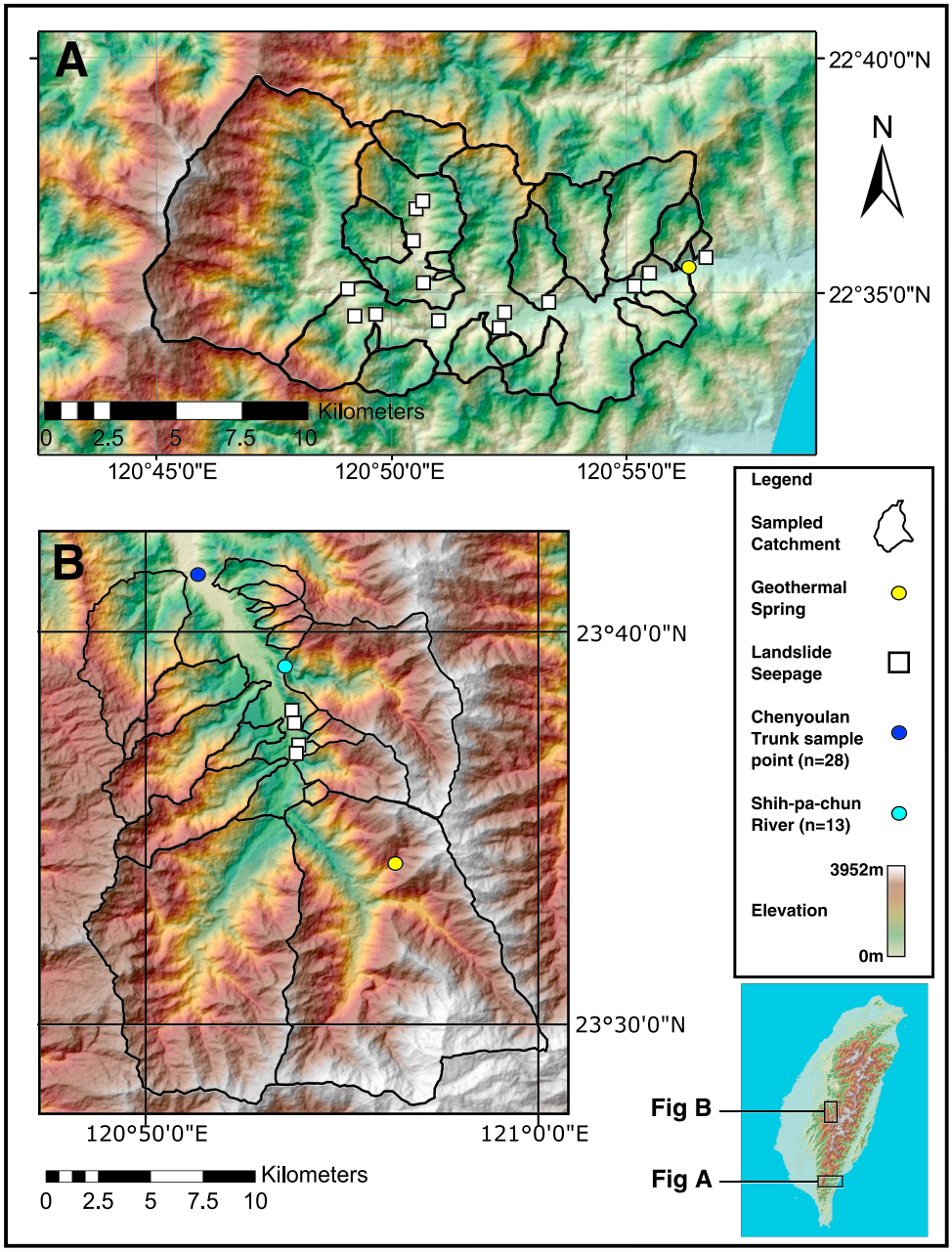

Figure 1. Location map of the sampled catchments and landslides in Taiwan from which seepage was collected. (a) Taimali River. (b) Chenyoulan River. Catchment maps are draped over a hillshade raster generated in ArcGIS workspace from NASA ASTER DEM data.

ratios of end-members in the WSA, which limits how much we can interpret from our measurements in terms of the balance of acids. This is particularly important since much of the calcite in the WSA is hydrothermally sourced (Jacobson et al., 2002), which often leads to highly enriched carbon isotope ratios (Galy & France-Lanord, 1999). Hence, these data are primarily used to support the more evolved analyses from the Taiwanese catchments.

3. Sample Processing

In most landscapes, acid is derived initially from dissolution of carbon dioxide in rain, which is then significantly supplemented by oxidation of organic matter in soils (Amundson, 2001; Jin et al., 2014; Solomon &

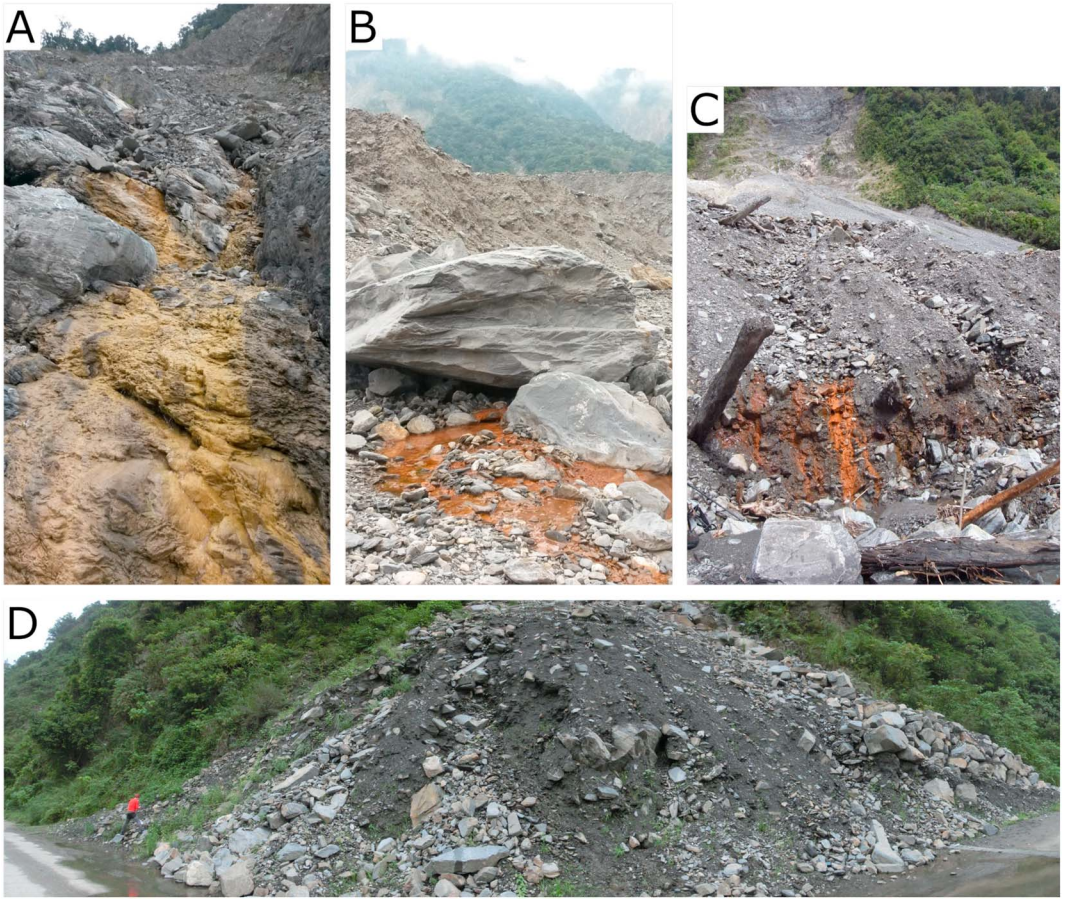

Figure 2. Landslide seepage sample sites in Taiwan and New Zealand. (a) Travertine formation on landslide seepage, Taimali River catchment (Taiwan). Travertine stain approx. 50 cm across. (b) Microbial growth in seepage exit point, base of giant landslide fan, Taimali River Catchment. Fan height (middistance) is approx 50 m. (c) Similar microbial growth in New Zealand landslide seepage sample. (d) Sample site at base of landslide deposit in Taiwan; note that all the fluid at the base of the landslide is from water exfiltrating from the deposit itself. Corresponding author for scale.

Cerling, 1987); in addition, oxidation of pyrite provides a source of sulfuric acid in the weathering zone (Brantley et al., 2013; Torres et al., 2016). Increased acidity of circulating fluids tends to increase weathering rates; in carbonate-dominated systems where weathering tends to be saturated with respect to calcite, increasing acidity increases the solubility of calcite and leads to buffering of pH by carbonate weathering (e.g., Hercod et al., 1998), while in settings where saturation is less important, increasing acid provides protons that accelerate hydrolysis. The products of silicate or carbonate weathering via carbonic acid in simple terms are dissolved cations and dissolved carbonate, the molecular form of which is determined by the pH. Clay minerals are a common further product, but since here we concern ourselves with the dissolved load of water in the landscape, we do not consider them. We measure the end products of the weathering, which, when combined with carbon isotope ratio measurements of the dissolved carbonate, allow us to estimate the sources of acid at the initial location of weathering.

Seepage samples were collected from the point at which the water exfiltrates from the landslide deposit, locations often clearly marked by co-associating bacterial colonies (see Figure 2). In some larger landslides, seepage is observed in multiple locations, and we collected fluid from the strongest flowing source. The drier weather conditions during our sampling periods precluded a systematic study of variability within specific landslide bodies. Stream samples were collected from the middle of channels to avoid sampling hyporheic water.

Major elemental data were analyzed to calculate both HCO_3^- and XSO_4^{2-}. Water samples were collected from source using an HDPE syringe, filtered on site using single-use 0.2 μm PES filters into several HDPE

bottles thoroughly rinsed with filtered sample water and one glass vial, also rinsed, for $\delta^{13}C_{DIC}$ analysis. Samples for cation analysis were acidified using ultrapure HNO_3^-. pH values were measured in the field at the time of sample collection. Analysis of cations was carried out using a Varian 720 ICP-OES, using SLRS-5 and USGS M212 as external standards, and GFZ-RW1 as an internal standard and quality control (QC). QC samples were included for every 10 samples to account for drift; no systematic drift was found, with random scatter less than 5%. Sample uncertainties were determined from calibration uncertainties and were always lower than 10% (see Tables S1–S3 in the supporting information for element-specific uncertainties). Anion analyses were performed using a Dionex ICS-1100 Ion Chromatograph, using USGS standards M206 & M212 as external standard and QC. Uncertainties were always less than 10% for each of the major anions (Cl^-, SO_4^{2-}, and limited NO_3^-). Bicarbonate (HCO_3^-) was calculated by charge balance; this has important implications for data interpretation, as discussed in detail below.

To measure the carbon isotope ratios in DIC, for each sample, an aliquot of between 0.2 and 2 ml of water, syringed directly from sealed tubes, was reacted with 3 drops of supersaturated orthophosphoric acid at 25 °C for at least 24 hr under a He atmosphere. A surplus of orthophosphoric acid was used to prevent fractionation of the evolved CO_2. We measured $\delta^{13}C_{DIC}$ on the evolved CO_2 using an autosampler Gasbench coupled to a Thermo Fisher MAT 253 Isotope Ratio Mass Spectrometer. We measured 10 repeats of the $\delta^{13}C_{DIC}$ of the evolved CO_2 by continuous flow IRMS. Commercially available spring waters "Thonon" and "Contrex" and synthetic calcium carbonate (Merck) were used as internal calibration and QC standards and are calibrated to international standards. Measurements were calibrated to V-PDB standard in per mille notation, and accuracy was always better than 0.5 per mille.

Suspended sediment from the Chenyoulan catchment was also assessed for elemental composition, amount of particulate carbonate, and its $\delta^{13}C$. These sediment samples were collected over the summer of 2010, during which the sampled sediment load varied between 0.1 g/L and above 200 g/L during passage of a large tropical storm in August. The samples were collected from a bridge near the outlet of the catchment, meaning the entire upstream area was represented in the suspended load. Samples were crushed to finer than 63 μm and analyzed using XRF; these data are reported in Table S6. To measure the carbonate content and its $\delta^{13}C$, we followed the same approach as the water samples, although samples were placed into tubes before ambient air was replaced with Helium. This method assumes that the only source of carbon in the suspended sediment is carbonate, which may introduce errors, as discussed below.

4. Uncorrected Results

In order to clarify the procedures adopted, we report the measured results before any correction is applied; derived results are reported after the correction methodology is described. Major elemental data and carbon isotope ratios for the samples are reported in Tables S1–S3, and all results below are reported in molar quantities or molar proportions unless otherwise stated. In the main trunk stream and the largest eastern tributary (the Shih-pa-chun River) in the Chenyoulan catchment, several repeat measurements were taken (n = 28 for main trunk, n = 13 for Shih-pa-chun), which do not show significant variability; for the sake of clarity these data are plotted as the average for each river in all figures. Overall, stream waters sampled in both catchments are broadly similar. The anion load is dominated by HCO_3^-, making up 30–48% of TDS in the Chenyoulan and Taimali; SO_4^{2-} forms around 15–25% in the Taimali and 8–25% in the Chenyoulan. Chloride is a minor component (<2%) reflecting relatively limited cyclic input to both catchments. In terms of cations, Ca^{2+} makes up 20–35% of TDS in the Taimali, similar to most streams in the Chenyoulan catchment, although in some western subtributaries, this proportion is nearer 15%. Smaller but still significant cation contributions are made up of Mg^{2+} (4–8% of TDS in Taimali, 5–10% in Chenyoulan) and Na^+ (4–5% of TDS in Taimali, 3–15% in Chenyoulan). Strontium and lithium concentrations are always below 1%.

In the seepage from landslides, higher TDS concentrations are observed than in any other surface waters, corresponding with other published locations (e.g., Emberson et al., 2015); TDS values of up to 65.9 mmol/L were found. However, in some sites with very high concentrations, the ratios of Na:Ca and Li:Ca are similar to hot spring waters, suggesting a deeper groundwater source underlying the landslide, and these are excluded from the later modeling. Excluding geothermal inputs is important, as our modeling assumes no

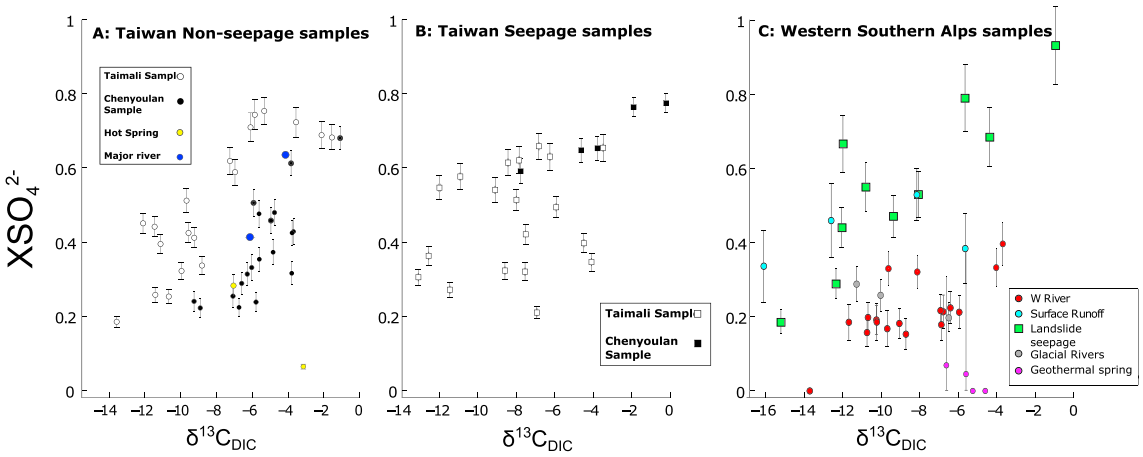

Figure 3. Carbon isotope ratio of dissolved inorganic carbon ($\delta^{13}C_{DIC}$) compared with the ratio of sulfate to bicarbonate contributions to anionic charge (XSO_4^{2-}, see equation (1) for definition). (a) Samples from Taiwan not sourced from landslide seepage, including Taimali and Chenyoulan rivers and geothermal springs. (b) Samples from Taiwan sourced from seepage from landslide deposits. (c) Samples from the Western Southern Alps of New Zealand. The error bars show the full analytical error attached to each measurement.

input of metamorphic CO_2. Within the remaining landslides, SO_4^{2-} is a larger proportion of TDS than in most streams (15–33%) and calcium is systematically also elevated (25–35% of TDS). The proportions of other elements are similar to those in the local streams, except for a few samples of seepage from landslides in the Taimali where magnesium or sodium is relatively elevated, although these seem uncorrelated to other values.

Measured values of $\delta^{13}C_{DIC}$ in Taiwanese streams vary from approximately −14‰ to 0‰. XSO_4^{2-} values range from 0.1 to 0.75. There is a general trend for a higher proportion of sulfate to correlate with more enriched values of $\delta^{13}C_{DIC}$ in both streams and rivers (Figures 3A and 3B), which is present in samples from both catchments. More enriched $\delta^{13}C_{DIC}$ and higher XSO_4^{2-} values are also often associated with the streams with more voluminous mass wasting (see Table S2 for landslide volumes in each catchment). The $\delta^{13}C_{DIC}$ in landslides is highly variable, between −13.1 and −0.2‰, with an average of −7.22‰. The XSO_4^{2-} values in landslide seepage are also similar to those measured in the streams (0.1–0.8), although in one case (TWS15–91), the measured sulfate was so high that the HCO_3^- calculated by charge-balance was negative, leading to XSO_4^{2-} greater than 1. It is unclear why this is the case; we have not persisted with modeling on this sample but do not exclude it from the sample set lacking a valid reason. Given overall similarity with other samples, a negative HCO_3^- value in TWS15–91 seems unlikely, and the measurement may represent effects we have not considered or constrained.

Figure 3c shows the same variables in the samples from the WSA. The samples from rivers tend to have systematically low XSO_4^{2-} values; this is also true of the majority of the landslides, with the exception of the Gaunt Creek landslide complex where the ratio is greater than 0.5 in some cases. The landslides demonstrate an extremely large range in the carbon isotope ratios; $\delta^{13}C_{DIC}$ varies between −19.30‰ and −0.95‰. This wide range is not just defined by different landslides—within the Gaunt Creek landslide complex, seepage $\delta^{13}C_{DIC}$ varies between −12.04‰ and −0.95‰ over a distance of only a few 100 m.

The XRF-derived elemental composition data of the suspended sediment from the Chenyoulan reflect varying contributions from silicate and carbonate rock, and we use these extrapolated trends to define the end-members for later analysis. The analyzed data are found in Table S6 in the data appendix; for the purpose of this study, we focus on the strontium:calcium and sodium:calcium ratios, which vary between 4.4×10^{-3} to 7.9×10^{-3} and 0.79 to 1.77 mol/mol, respectively. The carbonate content of these sediments ranges between 1.6 and 4.0%, and the associated values of $\delta^{13}C$ vary between −4.55‰ and −3.46‰, with a mean of 2.56 ± 0.62% and −4.01 ± 0.27‰ (1 standard deviation), respectively. We have exploited these measured values of suspended sediment to model the balance of substrates and solvent acids at the point of weathering for the sampled waters; this modeling is detailed in the following section.

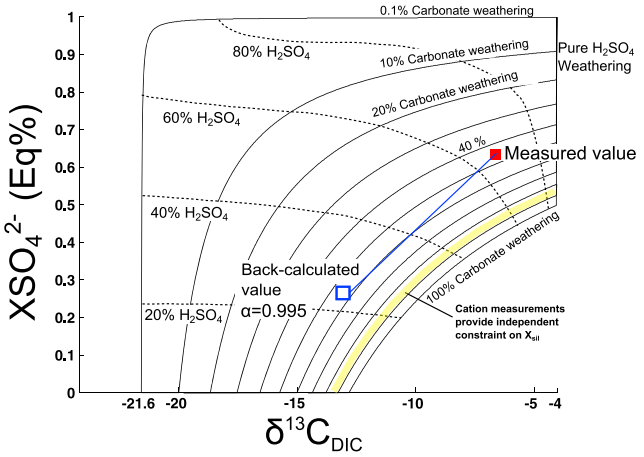

Figure 4. Diagram of the XSO_4^{2-} - $\delta^{13}C_{DIC}$ phase space, showing the contours of percentage of sulfuric acid driven weathering compared to carbonic acid driven weathering (dashed lines) and contours of percentage of carbonate weathered compared to silicate weathered. Adapted from Galy and France-Lanord (1999). We also show the approach to back-calculating the initial weathering state (blue square), starting with the measured value (red square) and using a value of alpha to approximate the cation-calculated fraction of silicate weathering (X_{sil}) as closely as possible—which defines an isoline, schematically shown in yellow with error margin.

5. Analysis

5.1. Modeling Approach

Our modeling aims to sequentially remove the effects of geothermal input, cyclic salt input, and secondary precipitation of calcite from the measured dissolved solutes. This should provide an improved estimate of the balance of solvent acids and substrates explicitly within the landslide deposits. We first briefly discuss why these sources impact XSO_4^{2-} and $\delta^{13}C_{DIC}$. Note that all of the code required for this analysis is publicly available via OpenScienceFramework (Emberson, 2018, https://osf.io/vnkxd/).

Dissolved inorganic carbon (DIC) in natural settings derives from a range of sources, but the primary inputs are from atmospheric CO_2, dissolution of carbonate, degassing of metamorphic CO_2, and oxidation of organic matter. The range of pH values measured at the sampled sites (7.02–8.67 in Taiwan, 6.87–8.43 in NZ) implies that the majority of DIC is in the form HCO_3^- (Zeebe & Wolf-Gladrow, 2001), and to reduce complexity in further calculations, we consider CO_2 and H_2CO_3 to be negligible. The isotopic compositions of carbon imparted by the different sources to the dissolved DIC are distinct. The marine sourced carbonate measured in the suspended sediment load of Chenyoulan River has a $\delta^{13}C$ of -4.01 ± 0.26‰. This is similar to the values obtained by studies elsewhere in Taiwan (-3‰, Hilton et al., 2010), which supports the use of this value also in the Taimali catchment. Organic carbon is significantly depleted in the heavy isotope, with carbon isotopic ratios generally close to -26‰ (Bird et al., 1994; Chiang et al., 2004; Hilton et al., 2010), and although this is fractionated kinetically during oxidation and diffusion in soils by approximately 4.4‰ (Cerling et al., 1991), organic carbon remains a depleted source of ^{13}C. Acknowledging the fractionation, we use a value of -21.6 ± 2‰ as the end-member value for carbonic acid in soil, where the associated error encompasses the majority of the published range in measurements.

As such, the $\delta^{13}C_{DIC}$ measured in sampled waters is affected by both the solvent (acid) and the substrate (carbonate). Increased carbonate weathering compared to that of silicate will move the $\delta^{13}C_{DIC}$ to less negative values, while weathering via carbonic acid derived from oxidation of organic material, as opposed to sulfuric acid derived from the oxidation of sulfide minerals such as pyrite, will pull the $\delta^{13}C_{DIC}$ value closer to -21.6‰. The balance of these forcings has previously been explored by Galy and France-Lanord (1999), and we demonstrate the mixing using a version of their diagram (Figure 4). The balance of acid can be estimated using $\delta^{13}C_{DIC}$ and XSO_4^{2-}, the sulfate proportion (Eq, %). Given values for XSO_4^{2-} and $\delta^{13}C_{DIC}$, we calculate the fraction of acids and substrates for any given point within the diagram. The analytical solution for these results is found in the openly accessible code available for this study (Emberson, 2018). Some areas are outside the phase space allowed by the end-members (Figure 4), and samples found within those areas demonstrate that we do not fully capture the complexity of the natural weathering system. Other end-members, such as ^{13}C-enriched metamorphic CO_2, are not accounted for, but our model attempts to explore the conceptually simpler carbonate-silicate substrate and sulfuric acid/organic sourced carbonic acid weathering system to first order. Here we note that since we lack constraints on the carbon isotope ratios of the end-members in the WSA we do not attempt to further correct these samples; all further analysis is of the better constrained Taiwanese samples.

5.2. Corrections

Several of the measured data points in Taiwan (Figures 3a and 3b) lie outside the mixing zone described by the initial weathering reactions. This can result from a number of effects; as mentioned above, other sources of carbon may complicate the analysis. We have tried to account for this. Degassing of metamorphic CO_2 would add a positive carbon isotope source to the DIC (e.g., Galy & France-Lanord, 1999; Shieh & Taylor, 1969). Himalayan springs have $\delta^{13}C_{DIC}$ values of as high as +10‰, and while the values we measure in geothermal springs (-7.04‰ in the Chenyoulan and -3.17‰ in the Taimali) are not as high, they still

must be accounted for. To reduce the complexity of analysis, we have attempted to exclude sources that could have nonnegligible deep groundwater input. The sampled hot springs provide a benchmark; the ratios of chemical elements in this water are very distinct, with high dissolved lithium/calcium and sodium/calcium ratios. In the Chenyoulan catchment, three of the landslide seepage samples have solute ratios very similar to the geothermal water, and although we include these data in the reported results, they are excluded from further analysis. This is particularly important since their enriched $\delta^{13}C_{DIC}$ values, likely due to metamorphic CO_2 degassing, lie outside the phase space defined by our $\delta^{13}C_{DIC}$ end-members, and as such would not yield usable results. In the Taimali, the hot spring waters are significantly more concentrated, and none of the landslides come close to the chemical signature of the local geothermal water (Li^+ concentrations are several orders of magnitude higher in the hot springs). While we acknowledge that this does not exclude a small amount of geothermal input to the seepage, we do not feel there is a justification for excluding any other samples on this account.

Rainfall in Taiwan can contain cyclic or pollutant derived solutes in concentrations that can impact the overall chemistry of the measured samples, particularly the XSO_4^{2-} due to release of sulfur by coal burning. To correct for these inputs, we use rainfall chemistry measurements. Wai et al. (2008) collected rainfall at Mt Lulin, which sits at the Southern end of the Chenyoulan catchment. Using their rainfall measurements in the Taimali catchment yields results of greater than 100% cyclic contribution for some elements (e.g., K^+). In the Taimali catchment we instead correct with seawater chemical ratios, with the exception of sulfate for which we use double the seawater SO_4^{2-}:Cl^- ratio, as suggested by Stallard and Edmond (1981). This is reasonable because of the proximity of the Pacific Ocean (<15 km). Using the ratios of Cl^- to major cations and anions (Ca^{2+}, K^+, Mg^{2+} and Na^+, and SO_4^{2-}) and assuming all Cl^- results from cyclic contribution, we removed cyclic cation contributions using the following standard equation:

$$[X]_{cyclic} = [Cl^-]_{sample} \times \left([X]_{rainfall}/[Cl^-]_{rainfall}\right), \quad (2)$$

where [X] is the measured concentration of any dissolved species. The assumption of all Cl^- from cyclic input is feasible as there are no evaporitic units reported in the sampled areas (Das et al., 2012, Central Geological Survey, M. of E. A., 2000), and geothermally sourced chloride would also provide elevated lithium values for which we have already accounted. We acknowledge that rainfall-sourced carbon can also impact the measured carbon isotope ratio. However, in prior studies, the proportion of carbon from rainfall is ~150–200 μmol/L (Fairchild et al. 1994), significantly below the approximate 10% error on the HCO_3^- concentration calculated by charge balance, since the latter is always much larger than the carbon that dissolves in rain in equilibrium with the atmosphere. Hence, we do not correct the carbon isotope ratios for the small cyclic input, but we note that metamorphic CO_2 may still affect the measured $\delta^{13}C_{DIC}$ The rainfall correction for major elements ensures, however, that the sulfate and calcium (in particular) that we discuss are primarily sourced from the dissolution of the rock mass itself.

Having corrected for other inputs, our model considers only the simplified system of carbon sourced either from oxidation of organic matter or carbonate rock. In this, postweathering effects—most importantly, the degassing of CO_2 from supersaturated water and precipitation of secondary carbonates, which both act to increase the XSO_4^{2-} and the $\delta^{13}C_{DIC}$—must be accounted for. Any link between intense weathering and increasing secondary precipitation will systematically affect estimates of weathering in mountain belts with extensive carbonate.

Both degassing and secondary precipitation fractionate carbon isotopes significantly, degassing with an isotopic fractionation factor (α), α = 0.992, precipitation with α = 0.998 (Friedman & O'Neil, 1977; Morse, 1983). These factors are derived for equilibrium fractionation, but we note that if the system is far from equilibrium (e.g., if samples are highly saturated with respect to atmospheric carbon dioxide) kinetic isotopic fractionation effects might also play a role in fractionation (e.g., Affek & Zaarur, 2014). We have no constraint on this.

In order to buffer the pH to near neutral values (in all streams pH > 8 and in seepage pH > 7.4), we expect that both degassing and secondary precipitation occur in concert, yielding an approximate intermediate α of 0.995. In order to estimate the initial weathering environment, and the associated acid balance, we need to back-calculate the initial values having accounted for the degassing and secondary precipitation.

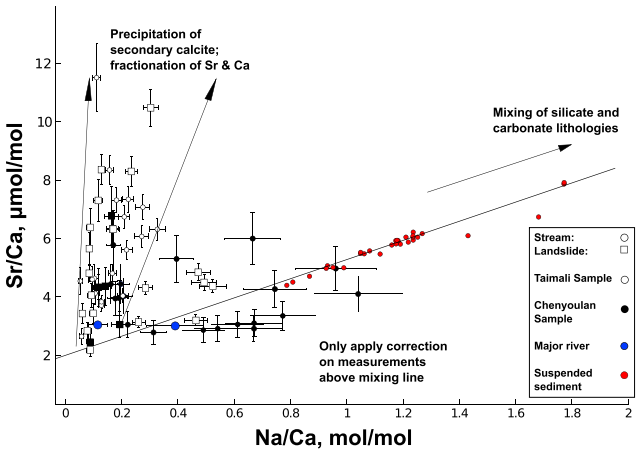

Figure 5. Ratio of sodium to calcium compared with the ratio of strontium to calcium in dissolved loads of the measured samples (before correction for secondary processes) as well as the suspended load (red circles) collected in the Chenyoulan catchment in 2010. The circles represent rivers, the squares landslide seepage. The filled symbols show results from the Chenyoulan catchment, and the empty ones from the Taimali. The sediment-defined silicate-carbonate mixing line is shown in black. Samples that are offset above this mixing line are interpreted to be subject to secondary calcite precipitation. This figure follows work by Bickle et al. (2015). The error bars capture the full analytical error for samples, except the two "major river" samples, which are the average of the series of samples collected at those two points; the error bars are 2 standard deviations of the averages.

We calculate the secondary precipitation and then estimate the initial values for $\delta^{13}C_{DIC}$ and XSO_4^{2-} based on this value. Following Bickle et al. (2015) and Albarede (1995), we estimate the precipitation of secondary calcite using a series of equations. Changes in Sr/Ca ratios through secondary precipitation are calculated first:

$$(Sr/Ca)_{measured} = (Sr/Ca)_0 {}^{*}\gamma^{(Kd-1)} \quad (3)$$

where $(Sr/Ca)_0$ is the initial value of Sr/Ca with no precipitation, γ is the fraction of original Ca remaining in the water, and Kd is the Sr/Ca molar partition coefficient for calcite. We use Kd = 0.05 (Bickle et al., 2015; Rimstidt et al., 1998); we lack constraints on the error associated with this value, but as pointed out by Bickle et al. (2015), the value calculated for γ is insensitive to the value of Kd while it remains small, and this is the assumption we adopt. The value chosen for $(Sr/Ca)_0$ depends on the relative contributions of silicate and carbonate to the initial weathering products. Previous studies (e.g., Bickle et al., 2015) have assumed that variations of Na/Ca and Sr/Ca ratios in riverine sediment are driven by variable input of silicate and carbonate end-members, and we follow the same procedure here (Figure 5). The higher Na^+:Ca^{2+} and Sr^{2+}:Ca^{2+} values in the suspended sediment collected from the Chenyoulan trunk stream in 2010 represent the more silicate derived sediment, and vice versa for the carbonate. A linear trend through the Na^+:Ca^{2+} and Sr^{2+}:Ca^{2+} in sediment extrapolated to where no sodium is present (the Y-intercept and thus the carbonate end-member) suggests that Sr^{2+}:Ca^{2+} of a catchment carbonate should be $2.08 \pm 0.18 \times 10^{-3}$ mol/mol. The silicate end-member Sr/Ca is chosen based on a Na/Ca value of 4, rather typical of silicate in active mountain belts (Calmels et al., 2011; Gaillardet et al., 1999; Galy & France-Lanord, 1999). An upper bound of 16.8 for the Na/Ca value can be estimated from the chemistry of the suspended sediment (XRF data in Table S6) and the amount of carbonate in the same samples approximated using the peak area of the carbon isotope signal. This assumes all the carbon derives from pure calcite, but such rough estimates imply a negative amount of CaO in the remaining silicate in two samples, demonstrating other contributors to the carbon—likely Dolomite. As such, we cannot use the peak area to make quantitative estimates of the error in the Na/Ca ratio; this is a potential source of model uncertainty, which could be better constrained in further study. The variability in lithology means that for a single sample, sediment mixed from sources across the whole catchment is unlikely to have perfect representation of these silicate or carbonate end-members. We feel that a generalized set of end-members is more appropriate than piece meal approach to individual samples; moreover, we lack sediment for each individual sample.

Figure 5 shows the relationship of the water samples with the sediment samples. Those samples that are close to or below the sediment-defined mixing line are assumed to have negligible secondary precipitation, while those that are offset above this line are interpreted to be affected by secondary precipitation (Bickle et al., 2015; Tipper et al., 2006). Some of the Chenyoulan tributaries sit below the trend defined by the sediment, likely due to mixing with a lower Sr/Ca silicate end-member, but since we have no constraint on this end-member we assume no secondary precipitation is occurring in these streams. Next, we calculate the amount of secondary precipitation required to return the samples to the sediment-defined trend:

$$Sr/Ca = A + B^{*}\,Na/Ca \quad (4)$$

where A and B are intercept and slope of the defined trend. Then, to find γ (equation (3)), we solve the following equation numerically:

$$Sr/Ca^{*}\,\gamma^{(1-Kd)} - A - B^{*}\,\gamma^{*}\,Na/Ca = 0 \quad (5)$$

Errors on this estimate are calculated using a Monte Carlo routine, where the final error is the standard deviation on 1,000 solutions to equation (5) where each variable has a pseudo randomly assigned

fraction of the total error attached to the measurement. A different set of pseudorandom numbers is used for each variable.

It is possible that the carbonate Sr/Ca end-member value may vary between catchments, but we suggest that since these are only first-order estimates of secondary precipitation, extrapolating from the Chenyoulan catchment to the Taimali catchment is justified, particularly given the overall similarity of the lithologies.

Using γ (equation (3)) to estimate the total amount of calcium dissolved in weathering fluid before secondary precipitation, we can for each sample estimate the proportion of silicate weathering (versus carbonate weathering) that led to the dissolved solute concentrations before any secondary precipitation occurred (cation-calculated X_{sil}). Some previous estimates of the fraction of weathering from silicate minerals in Taiwan have relied upon typical ratios of sodium and calcium in silicate minerals (Calmels et al., 2011); in order to compare our findings with these studies, we also use molar ratios, but with the recalculated calcium prior to loss to secondary precipitation.

The calculated value of γ also allows us to estimate the value of the initial HCO_3^- and $\delta^{13}C_{DIC}$ before secondary precipitation and associated degassing. The total carbon lost is a function of the calcium consumed by secondary precipitates. Assuming that the excess CO_2 evolved by carbonate precipitation is degassed, precipitation will mean two moles of carbon are degassed for each mole of precipitated calcium (equation (6)).

$$Ca^{2+} + 2HCO_3^- = CaCO_3 + H_2O + CO_2 \quad (6)$$

We make the simplifying assumption that the two processes have operated in equal proportion for each sample. However, CO_2 may degas from fluids that are supersaturated with respect to atmospheric CO_2 without precipitation of secondary calcite (e.g., Johnson et al., 2008; Wallin et al., 2013). We have no constraint on the magnitude of this degassing, and we can only correct for the change in DIC and $\delta^{13}C_{DIC}$ where we know the loss of calcium. This may be a source of error, which we discuss below.

As such, where we estimated γ values of less than 1 (i.e., secondary precipitation has occurred), we model the values of DIC and $\delta^{13}C_{DIC}$ before secondary precipitation using an α value of 0.995 (describing simultaneous degassing and secondary precipitation). The location of the "initial" sample in $XSO_4^{2-} - \delta^{13}C_{DIC}$ space can then be found, and an estimate of initial carbonate-silicate weathering ratio is possible based on this location (Figure 4). Here onward we refer to this as the "Isotope calculated X_{sil}." This can be compared with the Cation-calculated X_{sil}, for example, to help test whether an equal proportion of secondary precipitation and degassing is a justified assumption for each sample.

A discrepancy between the two estimates of X_{sil} could arise for a number of reasons, depending on whether the Cation-calculated or Isotope-calculated value is more silicate rich; this is discussed in more detail below in section 6.

5.3. Modeling Results

We report the results from each stage of the correction process for the Taiwanese samples, ending with the derived balance of acids in sampled sources, allowing comparison of different geomorphic settings. Having corrected for metamorphic and cyclic inputs (see notes in Table S2), the next step is the correction for secondary precipitation. Some tributaries from the Chenyoulan River are relatively well described by a mixing between silicate and carbonate end-members with no secondary effects. A few lie below the mixing trend, presenting no evidence for secondary precipitation (Figure 5). Elsewhere in the Chenyoulan catchment and in the majority of the Taimali catchment, tributaries are significantly offset above the mixing trend, suggesting that secondary precipitation is important. This is corroborated by field observations of extensive carbonate precipitation at sites of seepage and in small tributaries. Figure 6 shows the calculated values of γ for these streams and the seepage from the landslides compared to TDS values corrected for the lost calcium and bicarbonate (here referred to as TDS*). As much as 80% of initial calcium is lost in some streams, and similarly, many of the landslides also exhibit losses of up to 80% (i.e., low γ values). Some seepage samples, however, only have ~20% loss. Higher weathering rates (reflected by higher TDS* values) in general give rise to more extensive secondary precipitation (Figure 6).

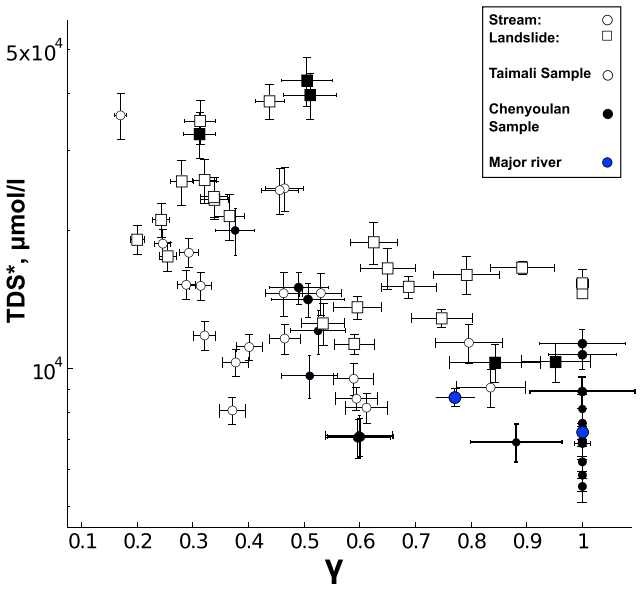

Figure 6. Comparison of the calculated value of γ (proportion of initially weathered calcium that is not lost to secondary precipitation) with the corrected value of total dissolved solids. The errors attached to γ are the standard deviation of a Monte Carlo simulation of errors, while the error bars on TDS* are the propagated errors on the summed initial TDS and the calculated lost calcium.

Some of the streams with relatively enriched measured $\delta^{13}C_{DIC}$ values have more carbonate-rich isotope-calculated X_{sil} values (Figure 7) than the cation-calculated X_{sil} values (i.e., the "initial" $\delta^{13}C_{DIC}$ is overly enriched in the heavy isotope compared to what would be expected based on Cation-calculated X_{sil}; see also Figure S3). These are mostly from the samples collected in the Chenyoulan catchment and particularly those where we calculated little or no loss of calcium through secondary precipitation. We suggest that degassing without secondary precipitation likely drives this; a loss of light carbon to the atmosphere enriches the remaining DIC on which we measure the isotope ratios. The precipitation of carbonate reduces the pH of the solution and without degassing it very quickly reaches conditions no longer favorable for precipitation without degassing. CO_2 degassing raises the pH value, and the range in pH (7.02–8.67 in Taiwan, 6.87–8.43 in NZ) suggests various degrees of incomplete degassing of the water. We have not constrained this, but where we calculated only limited secondary precipitation, this may be a significant loss of DIC before sampling. A true correction would therefore lead to an initial state that is more depleted in $\delta^{13}C_{DIC}$, which would more closely match the two estimates of carbonate and silicate weathering ratio.

On the other hand, some samples with more depleted initial carbon isotope ratios yield a more silicate rich isotope-calculated X_{sil} value compared to the cation-calculated X_{sil} values. For the most part these are samples from the Taimali catchment, and particularly samples of landslide seepage. One interpretation of both of these discrepancies is that the relative proportions of degassing and secondary precipitation are not equal, as our model assumes, or that $\delta^{13}C_{DIC}$ enriched CO_2 from metamorphic sources may play a larger role than we have assumed. In both cases, these discrepancies highlight the need for further study.

We measure the $\delta^{13}C_{DIC}$ on all of the dissolved carbon, but if our assumption that all carbon in the sample is HCO_3^- is wrong, then errors could result. For example, it is possible that excess dissolved CO_2 in the samples (i.e., degassing is not complete in the bottled samples) could lead to errors in the measured $\delta^{13}C_{DIC}$. This could occur because the depletion of $\delta^{13}C$ in dissolved CO_2 compared to dissolved HCO_3^- (Friedman & O'Neil, 1977) would lead to a more negative estimate of overall $\delta^{13}C_{DIC}$ than would fairly represent the HCO_3^- used to calculate XSO_4^{2-}. In addition, if a significant proportion of the carbon in solution is formed of ^{13}C depleted dissolved organic carbon (DOC) such as organic acids and that DOC gets oxidized by the acidification during the $\delta^{13}C_{DIC}$ determination, this could lead to underestimates of the $\delta^{13}C_{DIC}$. Published measurements of DOC in Taiwanese mountain rivers of between 0.5and 4 mg.l^{-1} during nontyphoon conditions (Kao & Liu, 1997) are similar to worldwide measurements (Ludwig et al., 1996). Such concentrations may be significant when compared to the charge balance estimates of HCO_3^-, of 13.9 to 213.6 mg L^{-1}, mean 38.6 mg L^{-1}. This remains an unconstrained source of error.

The factors that affect $\delta^{13}C_{DIC}$ as described above, as well as the variability on the $\delta^{13}C_{DIC}$ end-members, suggest that the isotope-calculated carbonate-silicate balance is likely less reliable than that derived from cations. However, despite the poor match between these estimates, we stress that the isotope-calculated estimate is at least improved by correcting for the secondary precipitation. This means the estimates of the initial acid balance are also improved by this correction.

We use the corrected values of XSO_4^{2-} and $\delta^{13}C_{DIC}$ to estimate the balance of acids. The correction for loss of calcium and DIC to precipitation of secondary calcite means the corrected values should be a better approximation of the initial weathering state within the water source. In sampled streams and rivers, the values are relatively consistent; in the Chenyoulan catchment carbonic acid makes up between 0 and 53% (average 28%) of the initial acid component (for the trunk stream and the Shih-pa-chun tributary values are taken as an average of the individual rivers), although only one stream—draining the easternmost part of the catchment—is ever below 10%. The average for the Chenyoulan trunk stream is 38%. In the Taimali catchment, the

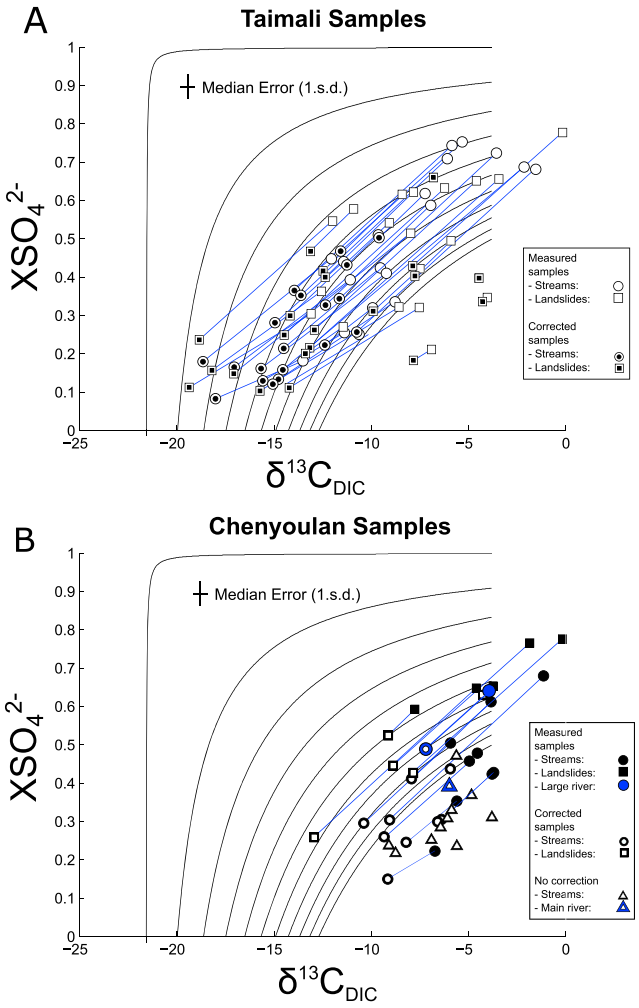

Figure 7. The estimated initial weathering states for samples from the (a) Taimali and the (b) Chenyoulan. The blue lines show the connections between the measured sample (more enriched carbon isotope value) and the calculated initial state based on an α value of 0.995. Streams in the Chenyoulan catchment without correction are denoted with triangles. The contour lines are the same as in Figure 4. Average errors are only shown to avoid cluttering of the figure, but errors for each sample are given in Tables S4 and S5.

carbonic acid contribution in the streams varies between 29 and 91%, with an average of 64%. The contribution of carbonic acid to the initial weathering in landslide seepage is broadly similar, albeit with a wider range; in the Chenyoulan catchment, it is between 6 and 61% (average 31%), while in the Taimali catchment, values are between 9 and 88% (average 54%). In each case, the contribution of sulfuric acid to this balance is the complement of carbonic acid input (i.e., 100 − X%). This demonstrates emphatically the importance of sulfuric acid; in seepage from landslides in the Chenyoulan catchment, anywhere between 39 and 94% of the acid is sulfuric, and the Taimali numbers (12–91%) are similarly considerable.

5.4. Impact on Carbon Cycle

For each sample we now have an estimate of the initial weathering state, which is the balance of silicate to carbonate substrate defined by the modal decomposition of the dissolved elements and corrected for secondary precipitation, and the balance of acids derived from the carbon isotope ratios and the relative proportions of anions (Figure 8). Using these estimates gives a first-order constraint on the impact of the weathering on the carbon cycle. Sulfuric acid driven weathering of silicates and carbonic acid-driven weathering of carbonates have no net effect on atmospheric CO_2. Therefore, the balance of sulfuric acid driven carbonate weathering to silicate weathering via carbonic acid determines the net drawdown of CO_2 from the atmosphere, and each variation of the acid-substrate reaction has a characteristic CO_2 output or drawdown. We calculate the net drawdown or evasion resulting from weathering both in landslide deposits and elsewhere (Tables S4 and S5) on the basis that sulfuric acid driven weathering of carbonate releases 1 mole of CO_2 to the atmosphere per mole of dissolved carbonate, and carbonic acid driven weathering of silicates consumes 1 mole of CO_2 for each mole of carbonic acid. Establishing the relative proportions of these two end-member reactions in our model results, we estimate the net modeled effect on atmospheric CO_2. In most measured samples, the fraction of carbonate weathering is so high that even small proportions of sulfuric acid drive a net outgassing of CO_2 into the atmosphere. In the Taimali streams, for each mole of weathered rock, there is an average of between 0.02 and 0.64 moles of CO_2 returned to the atmosphere; this is higher in landslide seepage samples, ranging from 0.08 to 0.86 moles. CO_2 outgassing tends to increase with increasing TDS values in both streams and landslide seepage. In the Chenyoulan catchment too, weathering results in net outgassing of CO_2, but there is no strong relationship between the TDS and the CO_2 export. Streams in the Chenyoulan catchment tend to release between 0.1 and 0.8 moles of CO_2 per mole of weathering; for landslide seepage this is between 0.35 and 0.88 moles. These outgassing estimates do not translate directly into changes in pCO_2 in the atmosphere, which depends on exchange with oceanic waters and the carbonate chemistry therein. As pointed out by Torres et al. (2016), oceanic carbonate burial on long time scales (but shorter than pyrite burial time scales—on the order of 10^7 years) will remove alkalinity and DIC from the ocean at a ratio of 2:1. Thus, atmospheric CO_2 will increase on long time scales if rivers deliver this at a ratio of less than 2; the acid-substrate balance that would lead to this is indicated in the inset to Figure 8, after Torres et al. (2016).

6. Discussion

Our analyses have allowed a description of the initial weathering state of sampled waters in two mountain catchments in Taiwan and the impact of this weathering on the carbon cycle. In the discussion below we

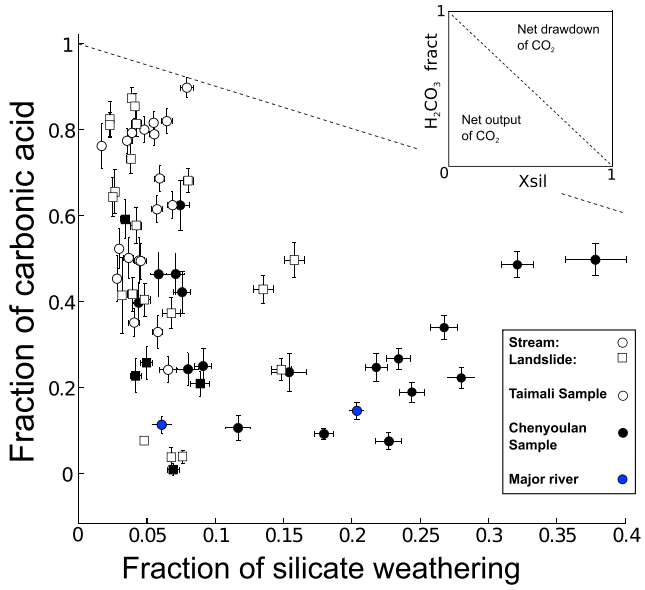

Figure 8. Cation-calculated fraction of silicate weathering compared to the estimate of the proportion of carbonic acid (compared with sulfuric acid) in Taiwanese samples. The errors attached to the cation-calculated fraction of silicate weathering are propagated through the calculation according to standard Gaussian propagation techniques. The error attached to the fraction of carbonic acid is calculated using a Monte Carlo technique as many of the variables that go into calculating it are not independent. Note that the error estimates here are for the modeling and should not be considered representative of natural variability. Inset: The overall picture of how the fraction of acid and silicate to carbonate affects the sequestration of CO_2.

determine to what extent our findings support our initial hypothesis: that weathering of labile phases in landslides can act as a primary source of CO2 in rapidly eroding mountain belts.

Before corrections are applied, the primary impression given by the measured data is a general trend of increasing XSO_4^{2-} with increasing $\delta^{13}C_{DIC}$, which is observed in both Taiwanese catchments (Figures 3a and 3b), as well as the WSA (Figure 3c). This can be interpreted in one of two ways. Either these measured results reflect the initial weathering state, with an increasing fraction of sulfuric acid leading broadly to more enriched $\delta^{13}C_{DIC}$ values, by reducing the carbonic acid input and/or increasing the fraction of carbonate weathered, or a relatively constant initial weathering state exists for all sources, with a varying degree of degassing and secondary precipitation, which would drive up both XSO_4^{2-} and $\delta^{13}C_{DIC}$. We have no a priori reason to prefer either of these explanations, which is why the correction for secondary precipitation and degassing is so important.

The modeled increase in secondary precipitation with increasing TDS (Figure 6)—which tends to collocate with highest measured XSO_4^{2-}, such as in the seepage from landslides—suggests that the second explanation posited above, in which the initial balances of acids and substrates are similar, is a good description of the initial weathering states, since a greater correction must be applied to settings with higher measured XSO_4^{2-}. Higher secondary precipitation where the weathering intensity is greater will lead to systematic underestimation of overall weathering in some settings. Where acid concentrations are greater and dissolution of carbonates is more intense, the circulating fluids will be further from equilibrium with the atmosphere with respect to dissolved carbon, leading to increased degassing and concurrent reprecipitation of carbonates. Even if the initial weathering state is unsaturated due to excess acidity, the degassing of CO_2 to the atmosphere will drive up the pH and supersaturate the water, leading to secondary precipitation. Hence, a correlation between increased TDS and increasing secondary precipitation is anticipated. However, it will also lead to a systematic underestimate of weathering, which worsens at higher weathering rates.

The variability of values of γ measured in landslide seepage suggests that flow paths within landslide deposits are not necessarily isolated from the atmosphere. Where extensive secondary precipitation has occurred, degassing must also have taken place, suggesting a significant exchange of CO_2 within some deposits. This could lead to cementation of landslide deposits with travertine, which we have observed in the field. On the other hand, field observation of gas bubbles forming in ponded seepage immediately at exfiltration points suggests that in many cases this subsurface degassing is not complete.

One of the key assumptions that goes into the estimates of initial acid balance is that the sulfuric and carbonic acids work with the same efficacy on both carbonate and silicate rock (e.g., if X_{sil} is 0.8, then it is 0.8 for both carbonic acid reactions and sulfuric acid reactions). This may not be the case in reality; in particular we note the work of Brantley et al. (2013), who show observations in upper parts of catchments of limited carbonate and sulfides, with both elevated at downstream locations, implying perhaps a greater proportion of carbonate dissolution by sulfide-derived acids. However, to maintain the simplicity of the analysis, we have adopted a model where the acids act in the same proportion on each substrate as one another. We have explored how the parameter space changes when this relative efficacy is altered; Figure S1 in the supporting information demonstrates that the isolines in $\delta^{13}C_{DIC}$ and XSO_4^{2-} space can vary widely but remain fixed at the axes by the input parameters. There is no convincing evidence provided by our measurements to support a difference in efficacy for either acid. This may be because landslides excavate below any sulfide-loss reaction fronts; we see no correlation between landslide size and dissolved sulfate (Figure S2), implying that the smaller slides share a similar weathering environment with the largest, which likely excavate several tens of

meters below the surface. Moreover, as pointed out by Torres et al. (2016), a difference in acid effect on each substrate will not change the overall effect on CO_2 consumption or release.

The discrepancy between cation-calculated and isotope-calculated values of X_{sil} suggests that we have not completely captured the complexity of the system in our modeling. The end-member estimates could be a source of error, but we suggest that the carbon isotope end-member ratios are relatively well defined in these catchments. Previous work in Taiwan has defined the organically derived CO_2 $\delta^{13}C$ (e.g., Chiang et al., 2004), and the analyzed suspended sediment gives a good constraint on the carbonate end-member, which also agrees with previous estimates elsewhere in Taiwan (Hilton et al., 2010). Any unconstrained degassing may be a significant source of this discrepancy as discussed above. Further, the isotope-calculated X_{sil} estimate relies on the assumption that the fraction of silicate to carbonate weathering does not vary between carbonic acid and sulfuric acid driven weathering, as well as the charge-balance calculated values for HCO_3^-.

Does this discrepancy matter? The location of the corrected samples in XSO_4^{2-}-$\delta^{13}C_{DIC}$ space is such that small changes in either $\delta^{13}C$ end-members or the amount of degassing can lead to significant discrepancies, similar to those we found, since this would generally move the samples relative to the *x* axis rather than the *y* axis. At lower XSO_4^{2-} values, where most samples end up after correction for secondary precipitation (Figure 7b), the shift relative to the *y* axis does not affect the estimate of the acid balance as much as the carbonate-silicate balance (see Figure 4). Hence, we suggest that the acid balance estimates are appropriate to first order.

The proportion of acids in landslide seepage varies widely, but the variability is also encompassed by the samples collected from streams where other fluid pathways—particularly through soils—are also important. This suggests that oxidation of organic material is as important, proportionally, in landslide deposits as in soil mantled hillslopes. Bearing in mind the first-order nature of the results, it is striking that the initial balance of acids is so similar between landslide seepage and the tributary streams draining soil-mantled subcatchments. Since we lack flux estimates for each flow path, we cannot definitively say which source has greater oxidation of organic matter per unit volume. Under the relatively dry sampled conditions, where dilution by rainfall is limited, the high overall solute concentrations (and therefore higher overall acid input) in seepage from landslide deposits suggest that water percolating in these deposits is exposed to more oxidation of organic matter compared to water in soil mantled zones. This suggests that the incorporation of macerated organic matter into landslide deposits (e.g., Fontaine et al., 2007; Hilton et al., 2011) is important in setting the conditions for weathering in these deposits, in addition to the documented role in the cycling of particulate organic matter (Hilton et al., 2008). The decomposition of this material is likely to occur in concert with microbial communities; recent work in Taiwan has shown that microbial decomposition of carbon in rocks in the east of Taiwan increases with erosion rate (Hemingway et al., 2018), which supports our findings here. If this is the case in sampled landslides, this implies that any inferred microbial communities are already well established in months to years after slope failure. Combined with the fact that the decomposition of organic matter is fast enough to sustain a significant source of isotopically depleted acid gives new insights into the organic processes governing weathering in mass wasting deposits, as well as emphasizing the importance of microbial activity in the weathering zone.

The $\delta^{13}C_{DIC}$ measured in samples from New Zealand helps underline the importance of acid derived from organic material in rapid weathering. These uncorrected samples can only offer partial support to findings from Taiwan; we lack constraint on the carbon isotope end-members, meaning the initial balance of acid is not simply constrained. Previous work using calcium isotopes has demonstrated that secondary precipitation of calcite is unlikely to be significant in this setting (Moore et al., 2013). Relatively radiogenic strontium isotope signatures in WSA carbonates point to extensive metamorphic exchange (Chamberlain et al., 2005; Jacobson et al., 2003; Templeton et al., 1998), which could introduce ^{13}C enriched CO_2 into the weathering system. Despite this, and the lack of secondary processes (which would also serve to increase the $\delta^{13}C_{DIC}$), seepage from landslide deposits in some cases still exhibits extremely low $\delta^{13}C_{DIC}$ values, in one case as low as −14.5‰. This suggests a ^{13}C depleted source of carbon, which is very likely to be organic material degradation. In comparison to other water sources in the WSA, the high solute concentrations in landslide seepage observed in concert with the depleted isotopic values (Figure 9) show quite how potent organic matter degradation can be for weathering. As in Taiwan, the carbon isotope values in landslide seepage are similar to those found in the rivers, suggesting an overall similar fraction of acid derived from organic

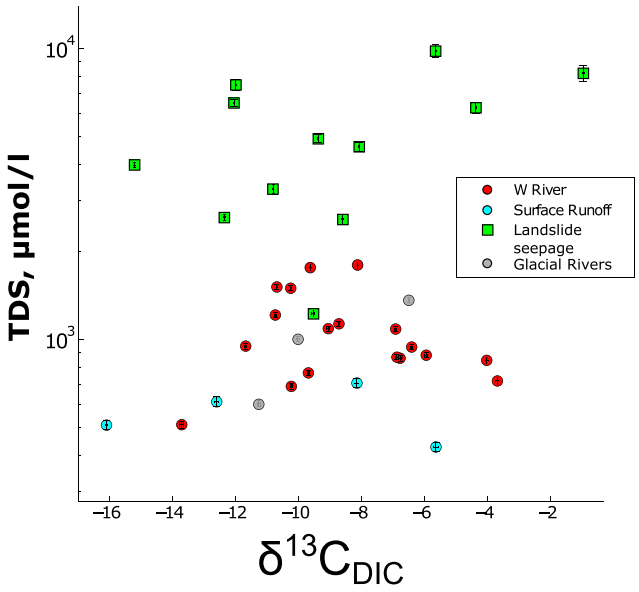

Figure 9. Plot of carbon isotope ratio of dissolved inorganic carbon ($\delta^{13}C_{DIC}$) compared with total dissolved solids in samples from the WSA in New Zealand. The errors attached to $\delta^{13}C_{DIC}$ encompass the full measurement error, while the error attached to TDS is the propagated error in the sum of the individual dissolved elements.

matter degradation in landslides and soil-mantled regions. And, as in Taiwan, the more accelerated weathering (higher TDS) in landslides suggests that this oxidation is more intense and provides a greater flux of acid than in soils.

Of further interest in the WSA samples is the local variability in $\delta^{13}C_{DIC}$ even within individual landslide deposits. We suggest that local pockets of degrading organic material within a deposit might act to create an aureole of rapid weathering. It is notable, however, that the $\delta^{13}C_{DIC}$ is not well correlated with the TDS values in the seepage, indicating that there may be other acid sources working in concert. High values of SO_4^{2-} in some of the landslide seepage samples could support a hypothesis of acid derived from sulfide mineral oxidation alongside organic material degradation. In the WSA the high solute concentrations in landslide seepage are derived from rapid weathering of small amounts of detrital carbonate; if this were not uniformly distributed among the rock mass in a landslide deposit, then highly variable $\delta^{13}C_{DIC}$ might be expected.

It is important to properly contextualize the acid derived from organic matter oxidation in the deposits of bedrock landslides within the larger carbon cycle. Carbonic acid driven weathering of silicates tends to draw down carbon dioxide from the atmosphere, but in each of the studied settings, the net sequestration of CO_2 that would result from this process is overwhelmed by the carbonate dominated weathering in landslides. Other studies have demonstrated how weathering of detrital calcite in the WSA prevents fast overall weathering there from serving as an effective drawdown for atmospheric CO_2 (Chamberlain et al., 2005; Jacobson et al., 2003). In a previous study we have shown that this is driven by weathering in landslide deposits (Emberson et al., 2016). In the two Taiwanese catchments we can take this further and suggest that the presence of sulfides in the bedrock combined with carbonate-dominated weathering acts as a source for carbon dioxide rather than a sink. Landslide deposits, where weathering is fastest, tend to be most pronounced sources for CO_2. This supports and adds substance to the suggestion of some authors (e.g., Torres et al., 2014, 2016) that erosion in some rapidly denuding mountain belts acts as a source for CO_2, rather than a sink, as has been previously assumed (e.g., Bickle, 1996; Raymo et al., 1988).

The persistence of this type of weathering over time will depend on how rapidly the oxidation of organic material and/or sulfides depletes the stock of these labile phases within the mobilized bedrock deposits. In the WSA, where the carbonate pool in the rock mass is rather limited, we demonstrated previously that the rapid weathering of detrital carbonate in landslide deposits decays over a decadal time scale (Emberson et al., 2016), and we anticipate that pyrite or organic matter will deplete in similar fashion (albeit over an unconstrained timescale) in Taiwanese landslides. If the decay is over a similar time span as the transient storage of material in the surface weathering zone, then an increase in mass wasting will fundamentally alter the long-term relationship between erosion and the drawdown of CO_2.

The importance of the physical process of landsliding in mobilizing both fossil and modern organic matter for transfer to sedimentary basins has been explored in previous studies (e.g., Hilton et al., 2008. West et al., 2011, Kao et al., 2014). This can lead to efficient burial of organic carbon, but it seems likely that landslide products that remain within the weathering zone—that is, within the source catchments or in transient storage centers—could negate this effect to some extent. Recent work has shown that in other catchments in Taiwan the oxidation of specifically fossil organic matter is not sufficient to outweigh the burial of organic matter offshore (Hilton et al., 2014), but to fully quantify the role of rapid erosion through mass wasting in the carbon cycle, a full census of the fluxes of both organic and inorganic carbon is necessary. The balance between degradation/oxidation of organic carbon, the resultant weathering, and final deposition/burial will depend on the sediment delivery ratios and storage time along the transport path of the mass wasting deposits, meaning that the impact of mass wasting on the organic carbon cycle is strongly dependent on both the erosional and transport history of sediment.

At this juncture it is important to consider how our modeling relates to the natural system. Through the course of our analysis, we have made a number of assumptions to simplify our model and corrections, which in combination mean our final results, and particularly estimates of effect on CO_2 (Figure 8), may differ from what is occurring in nature and should be considered as the beginning, rather than the end, of a research endeavor. Further study to clarify the importance of and variability in cyclic and metamorphic input of salts and carbon would help constrain our model, as would better constraints on the rates and proportions of degassing and precipitation, as both can influence the parameters of our model (e.g., DePaolo 2011). Furthermore, there are other factors that we do not consider as part of our model that play a role in natural weathering environments; the contribution of protons through oxidation of ferrous iron silicates may dissolve carbonate and influence the CO_2 budget (e.g., Buss et al., 2008; Fletcher et al., 2006), while the particular types and sources of organic acids additionally remain unconstrained. The natural weathering system is more complex than we have been able to simulate, but our results nevertheless pose pertinent questions that require further research to fully understand and answer.

7. Conclusion

We have used carbon isotope ratios and major dissolved elemental data from a range of landslides and rivers in the rapidly eroding mountains of Taiwan and New Zealand to demonstrate the importance of degradation of organic matter in producing the extremely elevated weathering rates observed in landslide deposits. The modeling of initial weathering conditions by removal of the effects of secondary precipitation and degassing allows us to see that the balance of acids in landslides is broadly similar to the local streams draining more soil-mantled settings. Given both the highly concentrated nature of landslide seepage, the similar balance of acids suggests that overall degradation of organic matter may be occurring proportionally faster in the fragmented and disordered landslide deposits than the soil-mantled landscapes nearby. Our uncorrected data from the WSA further suggest elevated degradation of organic matter. We also demonstrate that locations of accelerated weathering are systematically subject to higher fractions of secondary precipitation; where rivers are saturated with respect to calcite, this must be corrected for to avoid systematic underestimates of weathering rates. We have shown that understanding the links between erosion and weathering requires information both about the substrate being weathered and the sources of acid (e.g., Torres et al., 2014, 2016). Crucially, weathering in landslides in the sampled Taiwanese catchments serves as a source of carbon dioxide to the atmosphere, refuting the common assumption that erosion drives drawdown of CO_2. Despite acting as the chief process of erosion in active mountain belts, landsliding has only a limited effect on silicate weathering. The potential for a net outgassing of CO_2 from weathering in transiently stored deposits suggests that if erosion in mountain belts does control climate through the sequestration of CO_2, then it must occur through a different process link.

Acknowledgments

We thank Hongey Chen, Kao Shui-Ji, and Hsieh Meng-Long and students for assistance and local knowledge in Taiwan; Thomas Rigaudier for help with carbon isotope analyses at the CRPG; and Carolin Zorn and Jan Schuessler for help with major element analysis at the GFZ. All authors were involved in the design of the study and collection of samples; R.E. and A.G. made lab measurements; R.E. analyzed data; R.E. wrote the paper with significant input from all authors. The authors declare no conflicts of interest, financial or otherwise. All data to support this study can be found in the supplementary material; analytical code is available via OpenScienceFramework at https://osf.io/vnkxd/. Funding was provided through Helmholtz institutional funding at the GFZ Potsdam. We further thank two anonymous referees and the editor, whose input significantly improved our study.

References

Adams, P. W., & Sidle, R. C. (1987). Soil conditions in three recent landslides in southeast Alaska. *Forest Ecology and Management*, *18*(2), 93–102. https://doi.org/10.1016/03781127(87)90136-8.

Affek, H. P., & Zaarur, S. (2014). Kinetic isotope effect in CO2 degassing: Insight from clumped and oxygen isotopes in laboratory precipitation experiments. *Geochimica et Cosmochimica Acta*, *143*(August 2014), 319–330. https://doi.org/10.1016/j.gca.2014.08.005

Albarede, F. (1995). *Introduction to geochemical modeling*. Cambridge: Cambridge University Press. https://doi.org/10.1017/CBO9780511622960

Amundson, R. (2001). The carbon budget in soils. *Annual Review in Earth and Planetary Science*, *29*(1), 535–562. https://doi.org/10.1146/annurev.earth.29.1.535.

Bickle, M. J. (1996). Metamorphic decarbonation, silicate weathering and the long-term carbon cycle. *Terra Nova*, *8*(3), 270–276. https://doi.org/10.1111/j.1365-3121.1996.tb00756.x

Bickle, M. J., Tipper, E. T., Galy, A., Chapman, H., & Harris, N. (2015). On discrimination between carbonate and silicate inputs to Himalayan rivers. *American Journal of Science*, *315*, 120–166. https://doi.org/10.2475/02.2015.02

Bird, M. I., Haberle, S. G., & Chivas, A. R. (1994). Effect of altitude on the carbon-isotope composition of forest and grassland soils from Papua New Guinea. *Global Biogeochemical Cycles*, *8*(1), 13–22. https://doi.org/10.1029/93GB03487

Brantley, S. L., Holleran, M. E., Jin, L., & Bazilevskaya, E. (2013). Probing deep weathering in the Shale Hills Critical Zone Observatory, Pennsylvania (USA): The hypothesis of nested chemical reaction fronts in the subsurface. *Earth Surface Processes and Landforms*, *38*(11), 1280–1298. https://doi.org/10.1002/esp.3415

Buss, H. L., Sak, P. B., Webb, S. M., & Brantley, S. L. (2008). Weathering of the Rio Blanco quartz diorite, Luquillo Mountains, Puerto Rico: Coupling oxidation, dissolution, and fracturing. *Geochimica et Cosmochimica Acta*, *72*, 4488–4507. https://doi.org/10.1016/j.gca.2008.06.020

Calmels, D., Galy, A., Hovius, N., Bickle, M., West, A. J., Chen, M.-C., & et al. (2011). Contribution of deep groundwater to the weathering budget in a rapidly eroding mountain belt, Taiwan. *Earth and Planetary Science Letters*, *303*(1–2), 48–58. https://doi.org/10.1016/j.epsl.2010.12.032

Calmels, D., Gaillardet, J., Brenot, A., & France-Lanord, C. (2007). Sustained sulfide oxidation by physical erosion processes in the Mackenzie River basin: Climatic perspectives. *Geology*, *35*(11), 1003–1006. https://doi.org/10.1130/G24132A.1

Carey, A. E., Kao, S. J., Hicks, D. M., Nezat, C. A., & Lyons, W. B. (2006). The geochemistry of rivers in tectonically active areas of Taiwan and New Zealand. In S. D. Willett, N. Hovius, M. T. Brandon, & D. M. Fisher (Eds.), *Tectonics, climate and landscape evolution: Penrose Conference Series. Geological Society of America, Special Paper 398*, 339–351.

Casagli, N., Ermini, L., & Rosati, G. (2003). Determining grain size distribution of the material composing landslide dams in the Northern Apennines: Sampling and processing methods. *Engineering Geology*, *69*(1–2), 83–97. https://doi.org/10.1016/S0013-7952(02)00249-1

Central Geological Survey, M. of E. A (2000). Geologic map of Taiwan.

Cerling, T. E., Solomon, D. K. I. P., Quade, J. A. Y., & Bowman, J. R. (1991). On the isotopic composition of carbon in soil carbon dioxide. *Geochemica et Cosmochimica Acta*, *55*, 3403–3405. https://doi.org/10.1016/0016-7037(91)90498-T

Chamberlain, C. P., Waldbauer, J. R., & Jacobson, A. D. (2005). Strontium, hydrothermal systems and steady-state chemical weathering in active mountain belts. *Earth and Planetary Science Letters*, *238*(3–4), 351–366. https://doi.org/10.1016/j.epsl.2005.08.005

Chang, C. P., Angelier, J., & Huang, C. Y. (2000). Origin and evolution of a melange: The active plate boundary and suture zone of the Longitudinal Valley, Taiwan. *Tectonophysics*, *325*(1–2), 43–62. https://doi.org/10.1016/S0040-1951(00)00130-X

Chiang, P. N., Wang, M. K., Chiu, C. Y., King, H. B., & Hwong, J. L. (2004). Changes in the grassland-forest boundary at Ta-Ta-Chia long term ecological research (LTER) site detected by stable isotope ratios of soil organic matter. *Chemosphere*, *54*(2), 217–224. https://doi.org/10.1016/j.chemosphere.2003.07.005

Dadson, S. J., Hovius, N., Chen, H., Dade, W. B., Hsieh, M.-L., Willett, S. D., et al. (2003). Links between erosion, runoff variability and seismicity in the Taiwan orogen. *Nature*, *426*(6967), 648–651. https://doi.org/10.1038/nature02150

Das, A., Chung, C.-H., & You, C.-F. (2012). Disproportionately high rates of sulfide oxidation from mountainous river basins of Taiwan orogeny: Sulfur isotope evidence. *Geophysical Research Letters*, *39*, L12404. https://doi.org/10.1029/2012GL051549

DePaolo, D. J. (2011). Surface kinetic model for isotopic and trace element fractionation during precipitation of calcite from aqueous solution. *Geochimica et Cosmochimica Acta*, *75*(4), 1039–1056. https://doi.org/10.1016/j.gca.2010.11.020

Emberson, R. (2018, March 6). Emberson_2018_Landslide_AcidBalance_Code. Retrieved from osf.io/vnkxd

Emberson, R., Hovius, N., Galy, A., & Marc, O. (2015). Chemical weathering in active mountain belts controlled by stochastic bedrock landsliding. *Nature Geoscience* https://doi.org/10.1038/NGEO2600, *9*(1), 42–45.

Emberson, R., Hovius, N., Galy, A., & Marc, O. (2016). Oxidation of sulfides and rapid weathering in recent landslides. *Earth Surface Dynamics*, *4*(3), 727–742. https://doi.org/10.5194/esurf-4-727-2016

Fairchild, I. J., Bradby, L., Sharp, M., & Tison, J.-L. (1994). Hydrochemistry of carbonate terrains in alpine glacial settings. *Earth Surface Processes and Landforms*, *19*, 33–54. https://doi.org/10.1002/esp.3290190104

Fletcher, R. C., Buss, H. L., & Brantley, S. L. (2006). A spheroidal weathering model coupling porewater chemistry to soil thicknesses during steady-state denudation. *Earth and Planetary Science Letters*, *244*, 444–457. https://doi.org/10.1016/j.epsl.2006.01.055

Fontaine, S., Barot, S., Barré, P., Bdioui, N., Mary, B., & Rumpel, C. (2007). Stability of organic carbon in deep soil layers controlled by fresh carbon supply. *Nature*, *450*(08 November), 277–280. https://doi.org/10.1038/nature06275

Friedman, I., & O'Neil, J. R. (1977). Compilation of stable isotope fractionation factors of geochemical interest. In M. Fleischer (Ed.), *Data of geochemistry*, (Vol. 440, pp. 1–114). Washington, DC: K.K., Geological Survey.

Fuller, C. W., Willett, S. D., Hovius, N., & Slingerland, R. (2003). Erosion rates for Taiwan Mountain basins: New determinations from suspended sediment records and a stochastic model of their temporal variation. *The Journal of Geology*, *111*(1), 71–87. https://doi.org/10.1086/344665.

Gaillardet, J., Dupré, B., Louvat, P., & Allegre, C. (1999). Global silicate weathering and CO2 consumption rates deduced from the chemistry of large rivers. *Chemical Geology*, *159*. https://doi.org/10.1016/S0009-2541(99)00031-5(1-4), 3–30.

Galy, A., & France-Lanord, C. (1999). Weathering processes in the Ganges-Brahmaputra basin and the riverine alkalinity budget. *Chemical Geology*, *159*(1–4), 31–60. https://doi.org/10.1016/S0009-2541(99)00033-9

Geertsema, M., & Pojar, J. J. (2007). Influence of landslides on biophysical diversity—A perspective from British Columbia. *Geomorphology*, *89*(1–2 SPEC. ISS), 55–69. https://doi.org/10.1016/j.geomorph.2006.07.019

Hemingway, J. D., Hilton, R. G., Hovius, N., Eglinton, T. I., Haghipour, N., Wacker, L., et al. (2018). Microbial oxidation of lithospheric organic carbon in rapidly eroding tropical mountain soils. *Science*, *360*(6385), 209–212. https://doi.org/10.1126/science.aao6463

Henderson, R., & Thompson, S. (1999). Extreme rainfalls in the Southern Alps of New Zealand. *Journal of Hydrology (NZ)*, *38*(2), 309–330.

Hercod, D. J., Brady, P. V., & Gregory, R. T. (1998). Catchment-scale coupling between pyrite oxidation and calcite weathering. *Chemical Geology*, *151*(1–4), 259–276. https://doi.org/10.1016/S0009-2541(98)00084-9

Hilton, R. G., Gaillardet, J., Calmels, D., & Birck, J. L. (2014). Geological respiration of a mountain belt revealed by the trace element rhenium. *Earth and Planetary Science Letters*, *403*, 27–36. https://doi.org/10.1016/j.epsl.2014.06.021

Hilton, R. G., Galy, A., & Hovius, N. (2008). Riverine particulate organic carbon from an active mountain belt: Importance of landslides. *Global Biogeochemical Cycles*, *22*, GB1017. https://doi.org/10.1029/2006GB002905

Hilton, R. G., Galy, A., Hovius, N., Horng, M., & Chen, H. (2010). The isotopic composition of particulate organic carbon in mountain rivers of Taiwan. *Geochimica et Cosmochimica Acta*, *74*(11), 3164–3181. https://doi.org/10.1016/j.gca.2010.03.004

Hilton, R. G., Galy, A., Hovius, N., Horng, M. J., & Chen, H. (2011). Efficient transport of fossil organic carbon to the ocean by steep mountain rivers: An orogenic carbon sequestration mechanism. *Geology*, *39*(1), 71–74. https://doi.org/10.1130/G31352.1

Ho, C. S. (1986). A synthesis of the geologic evolution of Taiwan. *Tectonophysics*, *125*(1–3), 1–16. https://doi.org/10.1016/0040-1951(86)90004-1

Hovius, N., Meunier, P., Lin, C.-W., Chen, H., Chen, Y.-G., Dadson, S., et al. (2011). Prolonged seismically induced erosion and the mass balance of a large earthquake. *Earth and Planetary Science Letters*, *304*(3–4), 347–355. https://doi.org/10.1016/j.epsl.2011.02.005

Hovius, N., Stark, C., & Allen, P. (1997). Sediment flux from a mountain belt derived by landslide mapping. *Geology*, *25*(3), 231–234. https://doi.org/10.1130/0091-7613(1997)025<0231:SFFAMB>2.3.CO;2

Jacobson, A. D., Blum, J. D., Chamberlain, C. P., Craw, D. C., & Koons, P. O. K. (2003). Climatic and tectonic controls on chemical weathering in the New Zealand Southern Alps. *Geochemica et Cosmochimica Acta*, *6*(1), 29–46. https://doi.org/10.1016/S0016-7037(02)01053-0

Jacobson, A. D., Blum, J. D., Chamberlain, C. P., Poage, M. A., & Sloan, V. F. (2002). Ca/Sr and Sr isotope systematics of a Himalayan glacial chronosequence: Carbonate versus silicate weathering rates as a function of landscape surface age. *Geochimica et Cosmochimica Acta*, *66*(1), 13–27. https://doi.org/10.1016/S0016-7037(01)00755-4

Jin, L., Ogrinc, N., Yesavage, T., Hasenmueller, E. A., Ma, L., Sullivan, P. L., et al. (2014). The CO2 consumption potential during gray shale weathering: Insights from the evolution of carbon isotopes in the Susquehanna Shale Hills critical zone observatory. *Geochimica et Cosmochimica Acta*, *142*, 260–280. https://doi.org/10.1016/j.gca.2014.07.006

Johnson, M. S., Lehmann, J., Riha, S. J., Krusche, A. V., Richey, J. E., Ometto, J. P. H. B., & et al. (2008). CO2 efflux from Amazonian headwater streams represents a significant fate for deep soil respiration. *Geophysical Research Letters*, *35*, L17401. https://doi.org/10.1029/2008GL034619

Kao, S. J., Hilton, R. G., Selvaraj, K., Dai, M., Zehetner, F., Huang, J. C., et al. (2014). Preservation of terrestrial organic carbon in marine sediments offshore Taiwan: Mountain building and atmospheric carbon dioxide sequestration. *Earth Surface Dynamics*, *2*(1), 127–139. https://doi.org/10.5194/esurf-2-127-2014

Kao, S. J., & Liu, K. K. (1997). Fluxes of dissolved and nonfossil particulate organic carbon from an Oceania small river (Lanyang Hsi) in Taiwan. *Biogeochemistry*, *39*(5), 255–269. https://doi.org/10.1023/A:1005864605382

Kirschbaum, M. U. F. (1995). The temperature dependence of soil organic matter decomposition, and the effect of global warming on soil organic C storage. *Soil Biology and Biochemistry*, *27*(6), 753–760. https://doi.org/10.1016/0038-0717(94)00242-S

Larsen, I. J., Montgomery, D. R., & Korup, O. (2010). Landslide erosion controlled by hillslope material. *Nature Geoscience*, *3*(4), 247–251. https://doi.org/10.1038/ngeo776

Lin, C. W., Chang, W. S., Liu, S. H., Tsai, T. T., Lee, S. P., Tsang, Y. C., et al. (2011). Landslides triggered by the 7 August 2009 Typhoon Morakot in southern Taiwan. *Engineering Geology*, *123*(1–2), 3–12. https://doi.org/10.1016/j.enggeo.2011.06.007

Ludwig, W., Probst, J.-L., & Kempe, S. (1996). Predicting the oceanic input of organic carbon by continental erosion. *Global Biogeochemical Cycles*, *10*(1), 23–41. https://doi.org/10.1029/95GB02925

Millot, R., Gaillardet, J., Dupré, B., & Allègre, C. J. (2002). The global control of silicate weathering rates and the coupling with physical erosion: New insights from rivers of the Canadian shield. *Earth and Planetary Science Letters*, *196*(1–2), 83–98. https://doi.org/10.1016/S0012-821X(01)00599-4

Moore, J., Jacobson, A. D., Holmden, C., & Craw, D. (2013). Tracking the relationship between mountain uplift, silicate weathering, and long-term CO2 consumption with Ca isotopes: Southern Alps, New Zealand. *Chemical Geology*, *341*, 110–127. https://doi.org/10.1016/j.chemgeo.2013.01.005

Morse, J. W. (1983). The kinetics of calcium carbonate dissolution and precipitation. In *Reviews in Mineralogy and Geochemistry* (Vol. 11, pp. 227–264). https://pubs.geoscienceworld.org/msa/rimg/article-abstract/11/1/227/110528/the-kinetics-of-calcium-carbonate-dissolution-and?redirectedFrom=fulltext

Norris, R. J., & Cooper, A. F. (2001). Late Quaternary slip rates and slip partitioning on the Alpine Fault, New Zealand. *Journal of Structural Geology*, *23*(2–3), 507–520. https://doi.org/10.1016/S0191-8141(00)00122-X

Raymo, M. E., & Ruddiman, W. F. (1992). Tectonic forcing of Late Cenozoic climate. *Nature*, *359*(6391), 117–122. https://doi.org/10.1038/359117a0

Raymo, M. E., Ruddiman, W. F., & Froelich, P. N. (1988). Influence of late Cenozoic mountain building on ocean geochemical cycles. *Geology*, *16*, 649–653. https://doi.org/10.1130/0091-7613(1988)016<0649:IOLCMB>2.3.CO;2

Riebe, C. S., Kirchner, J. W., & Finkel, R. C. (2004). Sharp decrease in long-term chemical weathering rates along an altitudinal transect. *Earth and Planetary Science Letters*, *218*(3–4), 421–434. https://doi.org/10.1016/S0012-821X(03)00673-3

Rimstidt, J. D., Balog, A., & Webb, J. (1998). Distribution of trace elements between carbonate minerals and aqueous solutions. *Geochimica et Cosmochimica Acta*, *62*(11), 1851–1863. https://doi.org/10.1016/s0016-7037(98)00125-2

Shieh, Y. N., & Taylor, H. P. (1969). Oxygen and carbon isotope studies of contact metamorphism and carbonate rocks. *Journal of Petrology*, *10*(1594), 307–331. https://doi.org/10.1093/petrology/10.2.307

Solomon, D. K., & Cerling, T. E. (1987). The annual carbon dioxide cycle in a montane soil: Observations, modeling, and implications for weathering. *Water Resources Research*, *23*(12), 2257–2265. https://doi.org/10.1029/WR023i012p02257

Stallard, R. F., & Edmond, J. M. (1981). Geochemistry of the Amazon 1. Precipitation chemistry and the marine contribution to the dissolved load at the time of peak discharge. *Journal of Geophysical Research*, *86*, 9844–9858. https://doi.org/10.1029/JC086iC10p09844

Templeton, A. S., Chamberlain, C. P., Koons, P. O., & Craw, D. (1998). Stable isotopic evidence for mixing between metamorphic fluids and surface-derived waters during recent uplift of the Southern Alps, New Zealand. *Earth and Planetary Science Letters*, *154*(1–4), 73–92. https://doi.org/10.1016/S0012-821X(97)00143-X

Tipper, E. T., Bickle, M. J., Galy, A., West, A. J., Pomiès, C., & Chapman, H. J. (2006). The short term climatic sensitivity of carbonate and silicate weathering fluxes: Insight from seasonal variations in river chemistry. *Geochimica et Cosmochimica Acta*, *70*(11), 2737–2754. https://doi.org/10.1016/j.gca.2006.03.005

Torres, M. A., West, A. J., Clark, K. E., Paris, G., Bouchez, J., Ponton, C., et al. (2016). The acid and alkalinity budgets of weathering in the Andes-Amazon system: Insights into the erosional control of global biogeochemical cycles. *Earth and Planetary Science Letters*, *450*, 381–391. https://doi.org/10.1016/j.epsl.2016.06.012

Torres, M. A., West, A. J., & Li, G. (2014). Sulphide oxidation and carbonate dissolution as a source of CO2 over geological timescales. *Nature*, *507*(7492), 346–349. https://doi.org/10.1038/nature13030

Wai, K. M., Lin, N.-H., Wang, S.-H., & Dokiya, Y. (2008). Rainwater chemistry at a high-altitude station, Mt. Lulin, Taiwan: Comparison with a background station, Mt. Fuji. *Journal of Geophysical Research*, *113*, D06305. https://doi.org/10.1029/2006JD008248

Wallin, M. B., Grabs, T., Buffam, I., & Laudon, H. (2013). Evasion of CO2 from streams—The dominant component of the carbon export through the aquatic conduit in a boreal landscape. *Global Change Biology*, *19*, 785–797. https://doi.org/10.1111/gcb.12083

West, A. J., Galy, A., & Bickle, M. (2005). Tectonic and climatic controls on silicate weathering. *Earth and Planetary Science Letters*, *235*(1–2), 211–228. https://doi.org/10.1016/j.epsl.2005.03.020

West, A. J., Lin, C., Lin, T., Hilton, R. G., Liu, S., Chang, C., et al. (2011). Mobilization and transport of coarse woody debris to the oceans triggered by an extreme tropical storm. *Limnology and Oceanography*, *56*(1), 77–85. https://doi.org/10.4319/lo.2011.56.1.0077

Willenbring, J. K., & von Blanckenburg, F. (2010). Long-term stability of global erosion rates and weathering during late-Cenozoic cooling. *Nature*, *465*(7295), 211–214. https://doi.org/10.1038/nature09044

Willett, S. D., Fisher, D., Fuller, C. W., Yeh, E. C., & Lu, C. Y. (2003). Erosion rates and orogenic wedge kinematics in Taiwan inferred from apatite fission track thermochronometry. *Geology*, *31*(11), 945–948. https://doi.org/10.1130/g19702.1

Yu, S.-B., Chen, H.-Y., & Kuo, L.-C. (1997). Velocity field of GPS stations in the Taiwan area. *Tectonophysics*, *274*(1–3), 41–59. https://doi.org/10.1016/S0040-1951(96)00297-1

Zeebe, R. E., & Wolf-Gladrow, D. A. (2001). *CO2 in seawater: Equilibrium, kinetics, isotopes*, *Elsevier Oceanography Series* (Vol. 65). Amsterdam: Elsevier.